SHORELINE CHANGES BEHIND DETACHED BREAKWATER

By Daohua Ming[1] and Yee-Meng Chiew,[2] Member, ASCE

ABSTRACT: A series of experiments were conducted to study shoreline changes caused by the presence of a detached breakwater under the influence of pure wave action. The breakwater length, B, and its distance from the initial shoreline, X, were the two main parameters investigated. The study analyzes the effect of these two factors on shoreline changes. The experimental data show that (1) the size of a salient, X_s, increases with B, but decreases with X; and (2) the deposition area of the salient, A, increases with both B and X for $X \leq B$. However, further increase in X ($X > B$) will lead to a reduction in A. Based on the experimental results, the study proposes a criterion to demarcate the formation of a tombolo from that of a salient. The data also show that the width of the tombolo is directly proportional to B and inversely proportional to X. Finally, a new relationship for estimating the sand deposition area is obtained, and published data from the literature are used to verify the new relationship.

INTRODUCTION

The use of detached breakwaters for shoreline protection has increased substantially in the last two decades. They are generally constructed away from and parallel to the shoreline to dissipate wave energy and cause sand deposition in the sheltered area of the breakwater. Although numerous physical model tests have been conducted to study the phenomenon (Shinohara and Tsubaki 1966; Rosen and Vajda 1982; Mimura et al. 1983; Suh and Dalrymple 1987), the complicated hydrodynamics and sediment transport mechanism around the breakwater have not been fully understood. There is especially a lack of reasonable quantitative relationships to determine the salient size and sand deposition even for the case of a single detached breakwater.

Sediment transport behind a detached breakwater is affected by many factors, including sediment supply, sediment properties, wave characteristics, coastal zone topography, and breakwater configurations. However, the most pronounced factors appear to be the breakwater length and the distance of the breakwater to the initial shoreline. The objective of this paper is to examine the effect of these two parameters on the salient size and sand deposition area behind the breakwater.

EXPERIMENTAL SETUP, CONSIDERATIONS, AND RESULTS

The experiments were conducted in a wave basin that was 10 m long, 5 m wide, and 0.7 m high. Fig. 1 shows the layout of the test setup. A plunger-type wavemaker was used to generate monochromatic waves. Sponge was placed behind the wavemaker to minimize wave reflection. The 6 m long beach consisted of uniformly distributed sand with a median grain size of D_{50} = 0.25 mm. A 1-cm thick Perspex sheet was used as the breakwater in the experiments. Sponge was placed in front of the breakwater and gravel was placed on top of the sponge. The former acted to reduce wave reflection, while the latter served to prevent scour at the toe of the breakwater.

The response of shoreline changes behind a detached breakwater is a very slow process, and thus model test time must be long enough for the shoreline to reach equilibrium. In this study, a preliminary test was first carried out to determine the duration needed for the experiments. The test condition of the run was as follows: length of breakwater, B = 1.5 m; distance between breakwater and the undisturbed shoreline, X = 0.9 m; incident wave height, H_o = 5.0 cm; and incident wave period, T_o = 0.85 s. The test result showed that changes of the shoreline had become insignificant after approximately 15 h of continuous wave action. Another test (test 15 in Table 1), which lasted for 43 h, showed that only between 1 and 6 mm of additional shoreline changes had occurred as compared to the preliminary test (note that only X is different between these two tests). Therefore, 15 h was regarded as the test duration needed for the beach to reach equilibrium. Besides this, experimental observations on the shoreline development were also used as a basis to decide whether equilibrium had been reached. To this end, the following criteria were used to ascertain whether a shoreline has reached its equilibrium stage:

1. Waves are breaking simultaneously and normal to the shoreline.
2. Wave runup and rundown are perpendicular to the shoreline; i.e., they follow the same route and do not cause any longshore current.
3. There is no noticeable advancement or recession of the shoreline for a duration of 4 h.

In this study, the choice of the actual test duration was guided by the combination of the predetermined test duration of 15 h and experimental observations.

In total, 18 experiments were conducted in the study, and Table 1 summarizes the test conditions and results. All of the tests were performed with incident waves approaching normal to the longitudinal axis of the breakwater. The procedures of each experiment were as follows:

1. Mold the beach without the breakwater to a predetermined starting slope, and the shoreline is made as straight as possible.
2. Run waves for 5–12 h until an equilibrium beach is

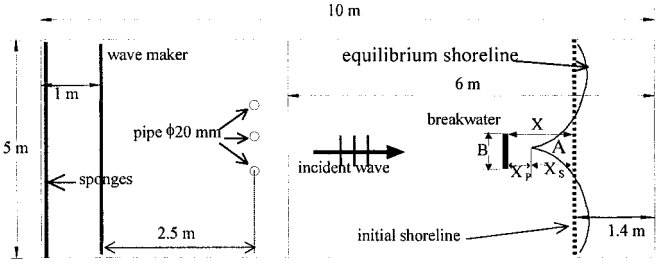

FIG. 1. Layout of Experimental Setup for Single Detached Breakwater

[1]Res. Fellow, Nat. Univ. of Singapore, Kent Ridge Crescent, Singapore 119260.

[2]Assoc. Prof., School of Civ. and Struct. Engrg., Nanyang Technol. Univ., Singapore 639798.

Note. Discussion open until September 1, 2000. To extend the closing date one month, a written request must be filed with the ASCE Manager of Journals. The manuscript for this paper was submitted for review and possible publication on August 5, 1998. This paper is part of the ***Journal of Waterway, Port, Coastal, and Ocean Engineering***, Vol. 126, No. 2, March/April, 2000. ©ASCE, ISSN 0733-950X/00/0002-0063–0070/ $8.00 + $.50 per page. Paper No. 18940.

TABLE 1. Test Conditions and Experimental Results

Test (1)	B (m) (2)	X (m) (3)	h_B (cm) (4)	X_b (m) (5)	H_o (cm) (6)	T_o (s) (7)	D (m) (8)	H_o/L_o (9)	T_d (h) (10)	X_s (m) (11)	A (m^2) (12)
1	0.90	0.60	6.00	0.50	5.00	0.85	0.335	0.044	18.0	0.600	0.240
2	1.20	0.60	6.00	0.50	5.00	0.85	0.335	0.044	18.0	0.600	0.461
3	1.50	0.60	6.00	0.50	5.00	0.85	0.335	0.044	18.0	0.600	0.515
4	0.60	0.90	8.00	0.50	5.00	0.85	0.335	0.044	18.0	0.240	0.138
5	0.90	0.90	8.00	0.50	5.00	0.85	0.335	0.044	17.0	0.624	0.403
6	1.20	0.90	8.00	0.50	5.00	0.85	0.335	0.044	19.0	0.900	0.482
7	1.50	0.90	8.00	0.50	5.00	0.85	0.335	0.044	19.0	0.900	0.557
8	0.60	1.20	10.00	0.50	5.00	0.85	0.335	0.044	18.0	0.120	0.058
9	0.90	1.20	10.00	0.50	5.00	0.85	0.335	0.044	18.0	0.500	0.253
10	1.20	1.20	10.00	0.50	5.00	0.85	0.335	0.044	18.0	0.804	0.591
11	1.50	1.20	10.00	0.50	5.00	0.85	0.335	0.044	20.0	1.200	0.620
12	0.60	1.50	12.00	0.50	5.00	0.85	0.335	0.044	17.0	0.040	0.014
13	0.90	1.50	12.00	0.50	5.00	0.85	0.335	0.044	16.0	0.340	0.185
14	1.20	1.50	12.00	0.50	5.00	0.85	0.335	0.044	18.0	0.600	0.481
15	1.50	1.50	12.00	0.50	5.00	0.85	0.335	0.044	43.0	0.940	0.967
16	1.00	0.50	5.00	0.50	5.00	1.15	0.370	0.024	21.0	0.500	0.231
17	1.00	1.40	11.00	0.50	5.00	1.15	0.370	0.024	21.0	0.560	0.242
18	1.00	1.40	11.00	0.50	6.00	1.15	0.370	0.029	21.0	0.520	0.270

formed. The resulting shoreline is referred to as the initial equilibrium shoreline (initial shoreline, in short).

3. Install the breakwater parallel to the shoreline, and at the predetermined distance (X) from the shoreline.
4. Remold the beach around the breakwater, which had been disturbed in step 3.
5. Start the formal experiment by running the same waves as in step 2.
6. Maintain constant mean water level, and monitor the transitional stages. Take pictures, and mark the progressing shoreline with small sticks.
7. Stop the wavemaker when the shoreline reaches equilibrium.

The symbols in Table 1 are defined as follows: H_o = deep water wave height; H_o/L_o = deep water wave steepness; h_B = water depth at the breakwater; T_o = wave period; L_o = deep water wavelength; D = water depth in the wave basin; T_d = test duration; B = length of the breakwater; X = distance of the breakwater to the initial shoreline; X_b = distance of the initial breaker line to the initial shoreline; X_s = distance of the salient apex to the initial shoreline; and A = plan area of sand deposition, namely the area enclosed by the initial shoreline and the shoreward equilibrium shoreline. Note that the shoreline refers to the still water line.

EXPERIMENTAL OBSERVATIONS

Fig. 2 shows how the diffracted waves approach the shoreline at an angle. As a result of this slanted wave approach, wave runup and rundown on the shoreline went along different routes. Wave runup was along the direction of the wave motion, while wave rundown was along the slope of the beach, as the latter was predominantly controlled by gravity. Observations showed that during one wave cycle, wave runup carried the sediment particles up the slope, while wave rundown carried them down the slope. Although sediment transport within one wave cycle was limited, the cumulative effect of sediment movement over time was both obvious and significant. The experimental data show that the salient formed could be as high as 3–5 cm above the still water level. This can only be explained by considering the runup and rundown motion. The motion of wave runup and rundown carried the sediment particles in a zigzag movement, with the net motion directed toward the centerline of the breakwater.

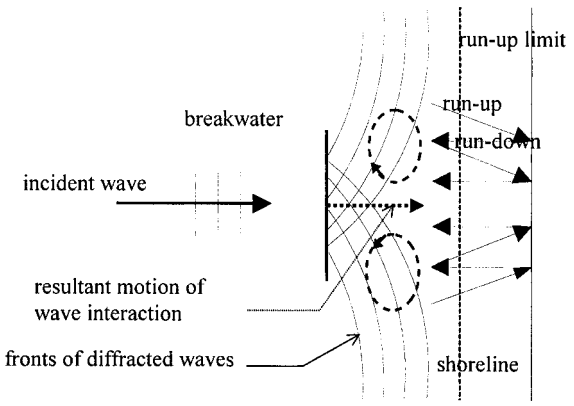

FIG. 2. Wave Interaction and Zigzag Movement of Sediment

Two circulation currents (Fig. 2) were formed behind the breakwater, and they carried the eroded sediment to the sheltered area behind the breakwater. The zigzag motion of the water body caused by wave runup and wave rundown contributed directly to the formation of the circulation currents. The zigzag motion resulted in two longshore currents that moved toward each other. They met at the breakwater centerline and turned toward the breakwater, resulting in the formation of the circulation current. It can also be inferred from observations that a secondary cause of the circulation currents was the gradient of the mean sea level between the illuminated area and the sheltered area. The difference is due to variations of the diffracted wave height.

Observations also showed that the fronts of the two diffracted waves met at the breakwater centerline. Fig. 2 illustrates how the waves interact behind the breakwater. Along the breakwater centerline, the wave interaction produced a combined motion perpendicular to the initial shoreline, which is opposite to the salient growth direction. It played a significant role in hindering the salient growth.

The rate of the salient growth was high initially, and it slowed down as equilibrium was approached. Finally at equilibrium, the waves reached the shoreline simultaneously and perpendicularly to it. Wave runup and rundown were along the same route, and there was no more zigzag movement of the sand, and hence no transport of sediment along the shoreline.

Generally, the size of a salient behind a breakwater is related to the two circulation currents, and the motion caused by wave interaction behind the center of the breakwater. The former facilitates growth of the salient, whereas the latter, which is opposite to the direction of the salient growth, deters its development. The strength of both of these currents depends on the breakwater length (B) and the distance of the breakwater to the initial shoreline (X). The effect of B and X on salient formation is discussed in the following section, and the data are presented in Figs. 3–6.

EFFECT OF BREAKWATER LENGTH (B)

Fig. 3 shows the influence of the length of the breakwater B on the salient size (X_s) and deposition area (A). In these tests, the distance of the breakwater to the original shoreline (X) as well as all of the other test conditions, including wave height, wave period, and beach slope, are kept constant. The data show that for a salient, X_s increases with B. This is because a large B significantly weakens wave interactions behind the breakwater, making the two circulation currents farther apart, thus favoring the growth of the salient. As B increases beyond a certain limit, the salient apex touches the breakwater, causing the formation of a tombolo. The data also show that A always increases with B.

Figs. 4(a–d) show the comparison of shoreline changes for varying breakwater length B while keeping X constant. Fig. 4(a) shows the shoreline changes of tests 1–3 for constant X at 0.6 m and varying B = 0.9, 1.2, and 1.5 m. Tombolos form for all three tests, but they differ in shape. The tombolo in test

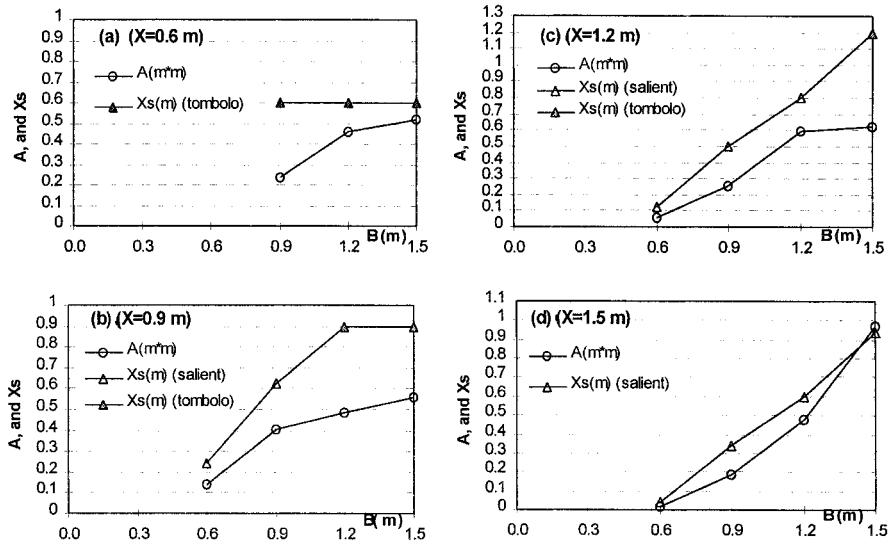

FIG. 3. Effect of Breakwater Length (B) on Deposition Area (A) and Salient Size (X_s)

3 is the widest, while that of test 1 is the narrowest. Generally, the data show that the longer the breakwater, the wider the tombolo.

Fig. 4(b) shows the shoreline changes of tests 4–7 for varying B = 0.6, 0.9, 1.2, and 1.5 m while keeping X constant at 0.9 m. In test 4 where X/B = 1.5, relatively strong wave interactions behind the breakwater were observed. As a result, a small salient with a relatively wide apex was formed. In test 5, X/B = 1.0, wave interactions were comparatively weaker, and consequently the salient apex was quite sharp, as shown in Fig. 4(b). Tombolos were formed in both tests 6 and 7, where X/B = 0.75 and 0.6, respectively. The tombolo of test 7 (with a larger B) was wider than that of test 6, similar to those observed in Fig. 4(a).

Fig. 4(c) shows the shoreline changes of tests 8–11 for varying B = 0.6, 0.9, 1.2, and 1.5 m while keeping X = 1.2 m. While salients were formed in tests 8–10, a tombolo was formed in test 11. In test 8 with X/B = 2.0, strong wave interactions behind the breakwater and weak circulation currents were observed in the experiment. As a result, the salient size of test 8 was only 0.12 m. A tombolo was formed in test 11, where X/B = 0.8. In this test, sediment deposition just reached the breakwater and the tombolo apex was narrow, indicating that the tombolo criterion occurs at approximately X/B = 0.8.

Fig. 4(d) shows the shoreline changes of tests 12–15 for varying B = 0.6, 0.9, 1.2, and 1.5 m while keeping X = 1.5 m. Note that only salient (and no tombolo) was formed in all of the tests. In test 12 where X/B = 2.5, experimental observations showed strong wave interactions behind the breakwater. It also showed that when the waves reached the shoreline behind the breakwater, they were almost perpendicular to the shoreline, and the circulation currents were very weak. As a result, the salient size of test 12 is only 0.04 m, which is the smallest among all of the tests conducted in this study.

EFFECT OF DISTANCE OF BREAKWATER TO INITIAL SHORELINE (X)

Fig. 5 and Figs. 6(a–d) show the effect of X on the salient size (X_s) and the deposition area (A) while B and all of the other test conditions remain constant. Fig. 5 shows that (1) the size of the salient decreases with X; and (2) an increase in X causes A to increase initially before it reaches its maximum at approximately $X = B$ [Figs. 6(c,d)]. However, further increment in X causes A to decrease.

Fig. 6(a) shows the shoreline changes for tests 4, 8, and 12 with varying X = 0.9, 1.2, and 1.5 m while keeping B constant at 0.6 m. In these three tests, $X/B > 1$, and only salients (and no tombolo) were formed. The data show that salient size X_s decreases with increasing X, as illustrated in Fig. 5.

Fig. 6(b) shows the shoreline changes for tests 1, 5, 9, and 13 with varying X = 0.6, 0.9, 1.2, and 1.5 m while keeping B constant at 0.9 m. For test 1 where X/B = 0.67, a tombolo was formed. In the other three tests, $X/B \geq 1$, and only salients were formed.

Figs. 6(c,d) show the shoreline changes for B = 1.2 m and 1.5 m, respectively. Tombolos were formed in tests 2, 3, 6, 7, and 11. In both of these figures, the data show that for the same B, the width of the tombolo is inversely proportional to X.

TOMBOLO CRITERION

Fig. 7 shows the experimental results plotted with X_s/B as a function of X/B. The data show that a tombolo is formed for $X/B \leq 0.8$. On the other hand, for $X/B > 0.8$, the data show the formation of salients. This trend reveals that X/B = 0.8 is the criterion for tombolo formation.

Previous researchers have proposed several tombolo criteria. For example, Gourlay (1981) suggested that $X/B < 0.5$ is the criterion for the formation of a double tombolo. Other criteria for a single tombolo include $X/B < 1.0–1.49$ [Gourlay (1981), experimental conditions], $X/B < 0.5$ (*Shore* 1984), $X/B < 0.5–0.66$ [Dally and Pope (1986), experimental conditions], and $X/B < 1.0$ [Suh and Dalrymple (1987), proposed for prototype conditions]. The tombolo criterion X/B = 0.8 obtained in the present study is within the range of these published results.

EMPIRICAL RELATIONSHIPS AND VERIFICATIONS

One of the main objectives of previous studies on shoreline changes behind a detached breakwater was to obtain quantitative relationships for design purposes. Among the parameters used to define such relationships are the volume of sediment deposition, and deepwater wave steepness, h_B, X_b versus X_s/X, X/B, or X_b/X.

Strictly speaking, the process of sand deposition behind a detached breakwater depends on several parameters, including the length of the breakwater (B), distance of the breakwater to the initial shoreline (X), wave conditions (H_o/L_o), sand size (D_{50}), sand density (ρ_s), beach slope (S), and others. However, apart from the geometric parameters of the breakwater, the other parameters such as H_o/L_o, D_{50}, and ρ_s are difficult to define and vary widely depending on the prototype conditions

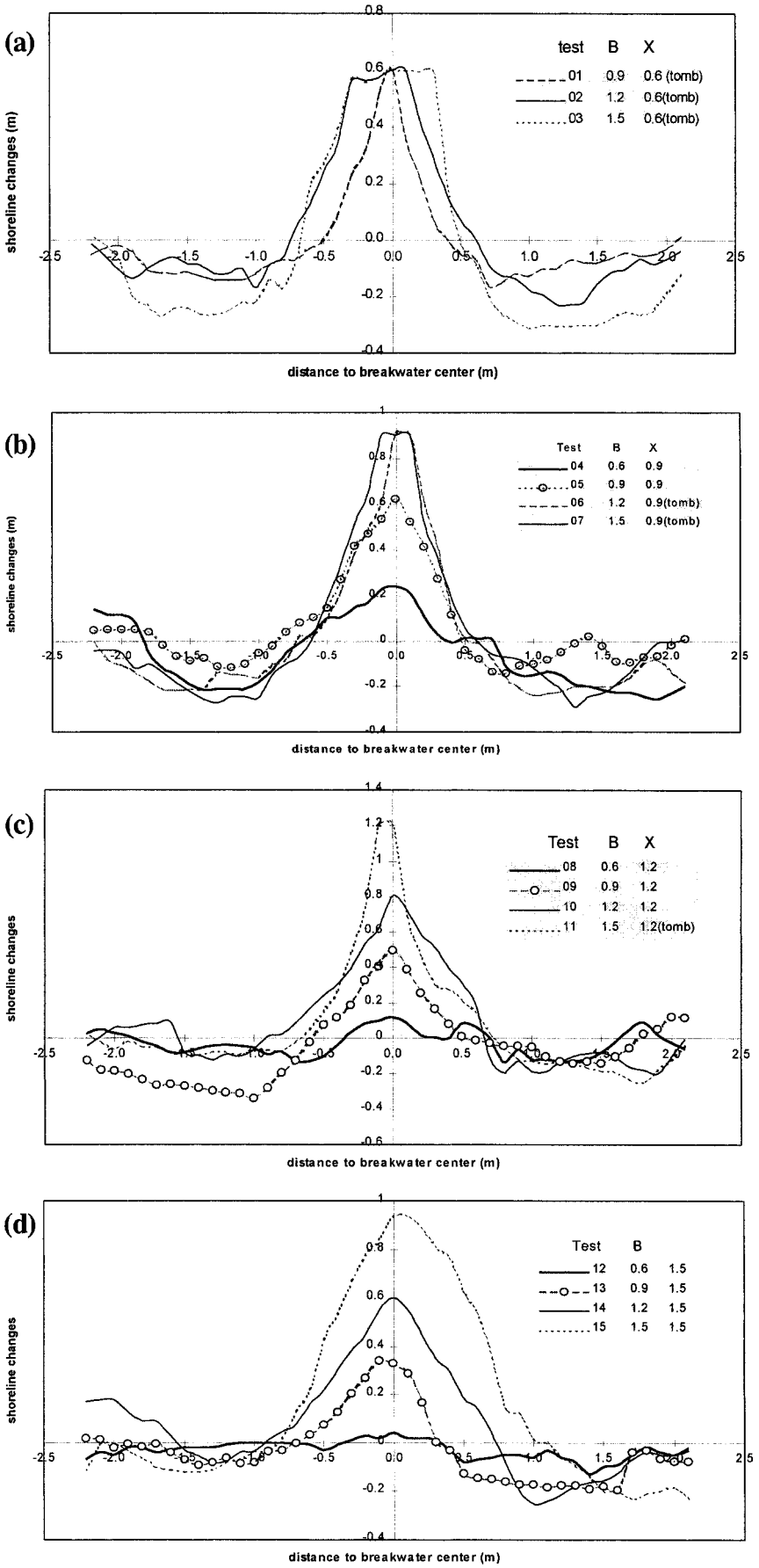

FIG. 4. Effect of Breakwater Length (*B*) on Shoreline Changes: (a) $X = 0.6$ m; (b) $X = 0.9$ m; (c) $X = 1.2$ m; (d) $X = 1.5$ m

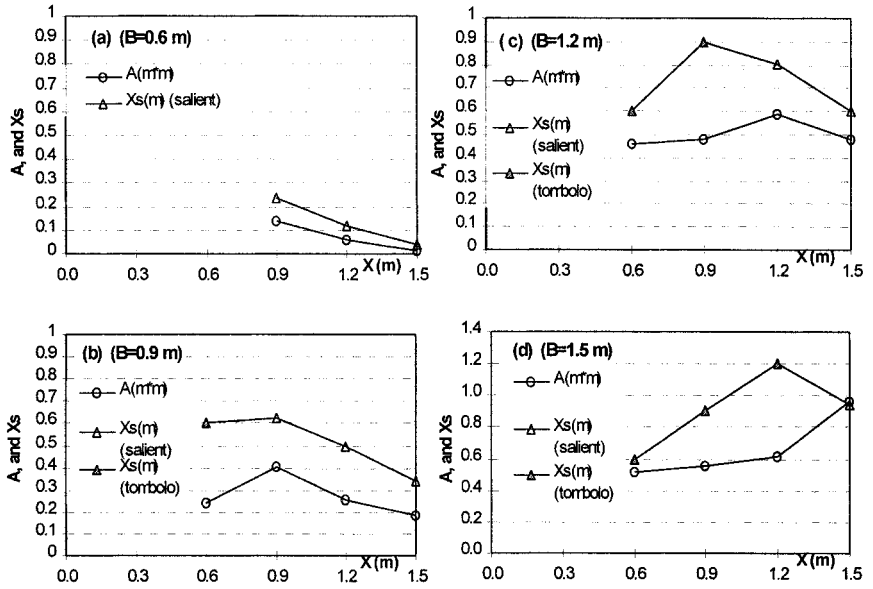

FIG. 5. Effect of Distance of Breakwater to Initial Shoreline (X) on Deposition Area (A) and Salient Size (X_S)

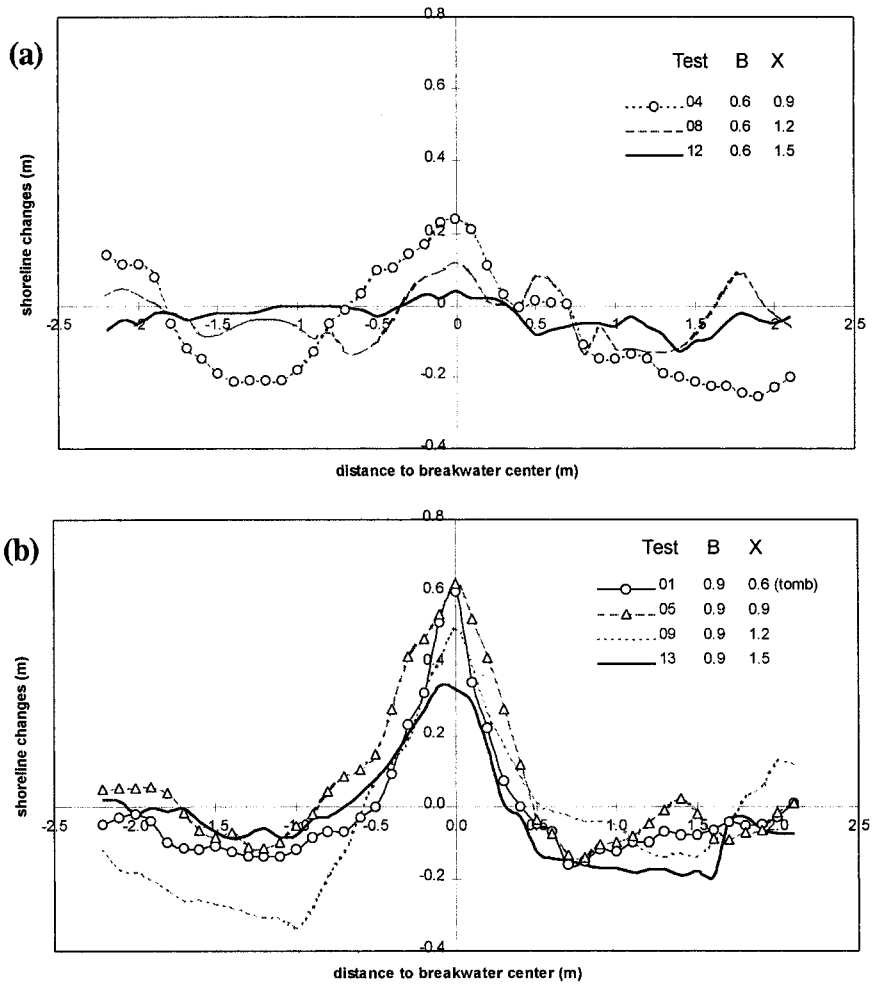

FIG. 6. Effect of Distance of Breakwater to Initial Shoreline (X) on Shoreline Changes: (a) $B = 0.6$ m; (b) $B = 0.9$ m; (c) $B = 1.2$ m; (d) $B = 1.5$ m

simulated in the experiments. In fact, existing experimental and prototype data appear to show that B and X are the primary parameters affecting the wave diffraction pattern, and hence sediment deposition behind a detached breakwater, whereas the other parameters are of secondary importance. Therefore, only B and X are considered in the present analysis.

The majority of researchers have attempted to use the length parameters such as X, B, X_p, and X_s to define the salient rela-

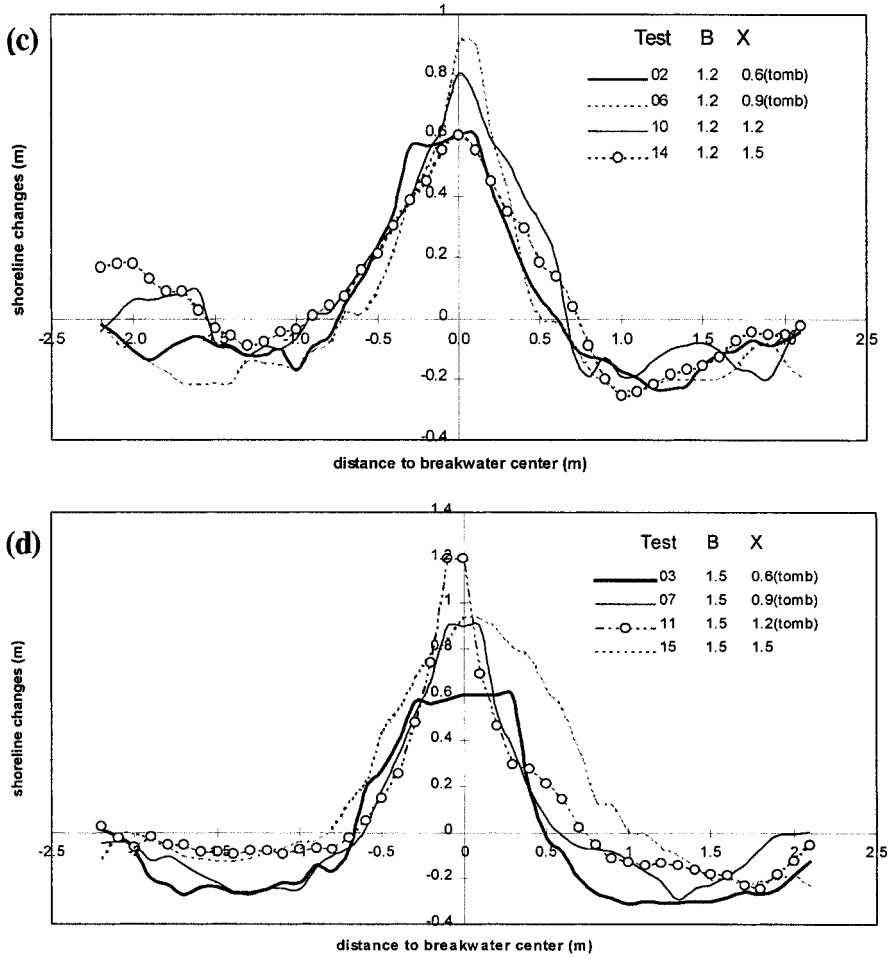

FIG. 6. (*Continued*)

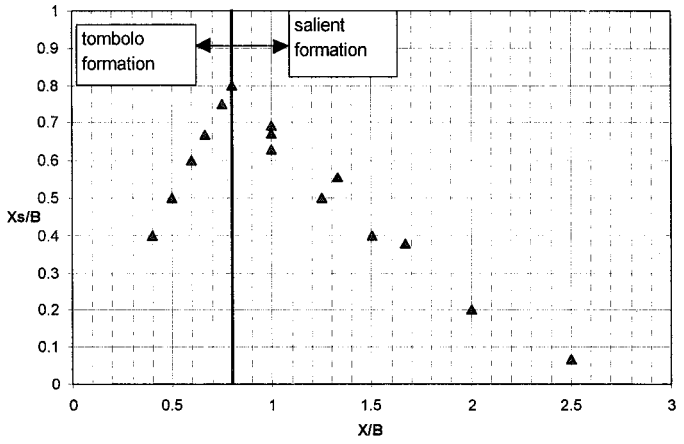

FIG. 7. Tombolo Criterion

tionship. However, such approaches usually suffer from data scattering (Hsu and Silvester 1990). On the other hand, other researchers have tried to relate these length parameters to the volume of sediment deposition (Harris and Herbich 1986; Suh and Dalrymple 1987). The accuracy of their fitted relationships suffers due to the limited data available. The detailed discussion of these approaches can be found in Ming (1997).

Apart from the two methods outlined above, the Japanese Ministry of Construction (*Handbook* 1986) employed a parameter known as salient area ratio (SAR) (salient area ratio = $A/\{BX\}$) to define sediment deposition behind a detached breakwater (Rosati and Truitt 1990). The Japanese Ministry of Construction (*Handbook* 1986) summarized its prototype breakwater project data by plotting SAR against B/X. The group reasoned that while one-dimensional parameters are not sufficiently indicative and descriptive, and three-dimensional parameters are difficult to obtain and measure, two-dimensional parameters appear more promising. However, no quantitative relationship is obtained by the Japanese Ministry of Construction for sand deposition area A and the two parameters B and X.

As was discussed earlier, the present data show that increasing B always results in more deposition, while increasing X would cause deposition to decrease if $X/B \geq$ approximately 1, or to increase if $X/B <$ approximately 1. Therefore, it would be appropriate to make A dimensionless by dividing it by $X^j B^k$, whereby j and k should satisfy the following conditions:

1. $j + k = 2$
2. Either $j > 0$, $k \leq 0$; or $j \leq 0$, $k > 0$

Condition 1 is to make A dimensionless, and condition 2 is to satisfy the data trend, which shows that X and B have opposite effects on A. Through numerous trials for different sets of j and k that satisfy the above conditions, the present study shows that X^2, corresponding to $j = 2$ and $k = 0$, appears to be the best. This set of j and k fitted well with the test data while offering reasonable physical meaning. Here, $A/(X^2)$ is the ratio of sand deposition area to the square of the distance of the breakwater to the initial shoreline, and X/B is the ratio of the distance of the breakwater to the initial shoreline. Fig. 8 shows the relationship of $A(X^2)$ and X/B for the experimental data of this study.

The equation of the curve in Fig. 8 is

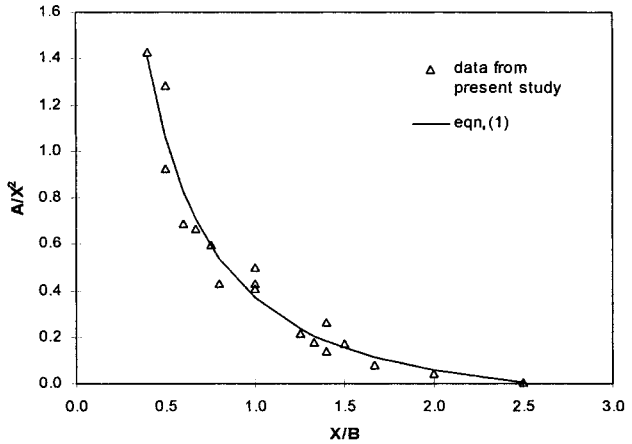

FIG. 8. Relationship of $A/(X^2)$ and X/B

$$\frac{A}{X^2} = -0.384 + 0.043\frac{X}{B} + 0.711\frac{B}{X} \quad (1)$$

and the correlation coefficient = 0.953.

The data show that when X/B is large, there would be a minimal or negligible shoreline response behind the breakwater. Nir (1982) stated that there is a minimal shoreline response when $X/B > 2.0$. The present study also shows that A/X^2 approaches zero when X/B is at 2.5. From a practical viewpoint, the applicability of (1) should be limited to $0.2 < X/B < 2.5$.

Eq. (1) is verified using the prototype data of the Japanese Ministry of Construction cited in Rosati and Truitt (1990). The graph in Rosati and Truitt (1990) was first digitized to obtain the data of $A/(BX)$ and the corresponding (B/X) values. The following relationship was used to determine $A/(X^2)$ in order to plot Fig. 9:

$$\frac{A}{X^2} = \frac{A}{BX} \times \frac{B}{X} \quad (2)$$

Fig. 9 shows the prototype data of the Japanese Ministry of Construction plotted as A/X^2 versus X/B. Eq. (1) is also superimposed on the figure for comparison, and the results show that the prototype data fit well with the proposed equation.

The experimental data of Rosen and Vajda (1982) and Shinohara and Tsubaki (1966) were also used to verify (1). These researchers have presented their results with graphs depicting the plan shapes of the shorelines. In the present study, their graphs were first digitized, and then the deposition areas were calculated using the digitized data. Fig. 10 shows the comparison of (1) with their experimental data. Eq. (1) agrees better with the data of Rosen and Vajda (1982) than with those of Shinohara and Tsubaki (1966). Even though the experimental condition of Shinohara and Tsubaki is similar to that in the present study in terms of wave steepness (0.019–0.046 for Shinohara and Tsubaki; 0.029–0.044 for the present study) and sand size (D_{50} = 0.3 mm for Shinohara and Tsubaki; D_{50} = 0.25 mm for the present study), their test duration was only 4–8 h. According to the experience gained in the present study, 4–8 h is too short for the beach to reach equilibrium. Although test durations were not shown in the paper of Rosen and Vajda (1982), the salient shapes presented by them tend to show that equilibrium has been reached. In contrast, the profile shapes of some salients in Shinohara and Tsubaki (1966) are flat and appear not to be in equilibrium. This probably explains why some of the data of Shinohara and Tsubaki (1966) fall below (1).

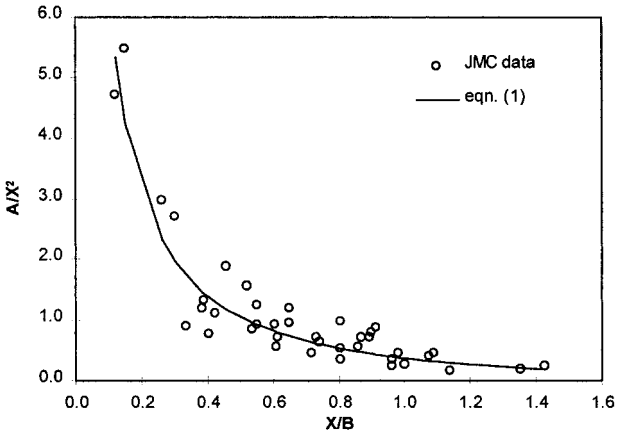

FIG. 9. Verification of (1) with Prototype Data of Japanese Ministry of Construction

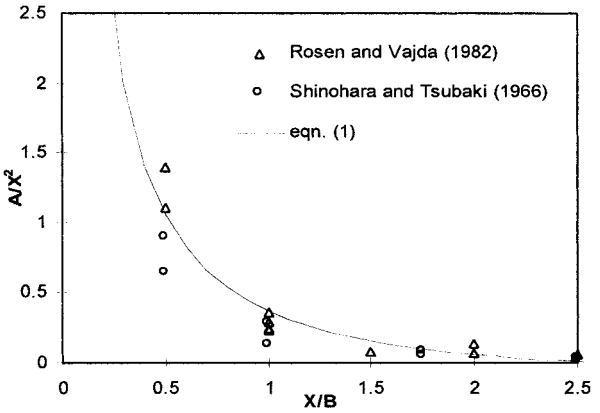

FIG. 10. Verification of (1) Using Experimental Data of Rosen and Vajda (1982) and Shinohara and Tsubaki (1966)

CONCLUSIONS

The study presents the results of a series of experiments conducted for shoreline changes behind a detached breakwater for different breakwater lengths (B) and distance of the breakwater to the initial shoreline (X). The data show that the size of a salient, X_s, increases with the length of the breakwater, B, but decreases with the distance between the breakwater and the initial shoreline, X. The deposition area of the salient, A, increases with both B and X. However, a further increase in X ($X > B$) will lead to a reduction in A.

The study also proposed an empirical criterion at $X/B = 0.8$ to demarcate the formation of a tombolo from that of a salient behind detached breakwaters. The experimental data show that the width of a tombolo is directly related to B and inversely proportional to X. Finally, existing methods relating the salient size to B and X are discussed, and a new equation [(1)] relating the sand deposition area behind the breakwater to B and X is proposed. The equation is verified with available published experimental and prototype data.

APPENDIX I. REFERENCES

Dally, W. R., and Pope, J. (1986). ''Detached breakwaters for shore protection.'' *Tech. Rep. CERC-86-1*, U.S. Army Engineers Waterways Experiment Station, Vicksburg, Miss.

Gourlay, M. R. (1981). ''Beach processes in the vicinity of offshore breakwaters.'' *Proc., 5th Australian Conf. on Coast. and Oc. Engrg.*, Institution of Engineers, Australia, 129–134.

Handbook of offshore breakwater design. (1986). River Bureau of the Japanese Ministry of Construction, Tokyo.

Harris, M. M., and Herbich, J. B. (1986). ''Effects of breakwater spacing on sand entrapment.'' *J. Hydr. Res.*, 24(5), 347–357.

Hsu, J. R. C., and Silvester, R. (1990). ''Accretion behind single offshore breakwater.'' *J. Wtrwy., Port, Coast., and Oc. Engrg.*, ASCE, 116(3), 362–380.
Mimura, N., Shimizu, T., and Horikawa, K. (1983). ''Laboratory study on the influence of detached breakwater on coastal change.'' *Proc., Coast. Struct. '83*, ASCE, Reston, Va., 740–752.
Ming, D. H. (1997). ''Modeling of sediment transport in the presence of breakwaters,'' PhD thesis, Nanyang Technological University, Singapore.
Nir, J. (1982). ''Offshore artificial structures and their influence on the Israel and Sinai Mediterranean beaches.'' *Proc., 18th Conf. on Coast. Engrg.*, ASCE, Reston, Va., 1837–1856.
Rosati, J. D., and Truitt, C. L. (1990). ''An alternative design approach for detached breakwater projects.'' *Miscellaneous Paper CERC-90-7*, U.S. Army Corps of Engineers Coastal Engineering Research Center.
Rosen, D. D., and Vajda, M. (1982). ''Sedimentological influences of detached breakwaters.'' *Proc., 18th Int. Conf. on Coast. Engrg.*, ASCE, Reston, Va., 1, 1930–1949.
Shinohara, K., and Tsubaki, T. (1966). ''Model study on the change of shoreline of sandy beach by the offshore breakwater.'' *Proc., 10th Int. Coast. Engrg. Conf.*, 551–563.
Shore protection manual, 4th Ed. (1984). U.S. Army Engineers Waterways Experiment Station, Coastal Engineering Research Center, U.S. Government Printing Office, Washington, D.C.
Suh, K., and Dalrymple, R. A. (1987). ''Offshore breakwaters in laboratory and field.'' *J. Wtrwy., Port, Coast., and Oc. Engrg.*, ASCE, 113(2), 105–121.

APPENDIX II. NOTATION

The following symbols are used in this paper:

A = plan area of sand deposition (namely, area enclosed by initial shoreline and shoreward equilibrium shoreline); shoreline refers to still water line;
B = length of breakwater;
D = water depth in wave basin;
D_{50} = median grain size of bed sediment;
H_o = deep water wave height;
H_o/L_o = deep water wave steepness;
h_B = water depth at breakwater;
L_o = deep water wavelength;
S = beach slope;
T_d = test duration;
T_o = wave period;
X = distance of breakwater to initial shoreline;
X_b = distance of initial breaker line to initial shoreline;
X_s = distance of salient apex to initial shoreline; and
ρ_s = sand density.